Bull. Chem. Soc. Jpn., 77, 1855–1859 (2004) 1855

Effect of Catalytic and Electrochemical Acetone Hydrogenation on the I–V Characteristics of an Acetone/Hydrogen-Based Thermally Regenerative Fuel Cell

Yuji Ando,* Yukihiro Aoyama,[1] Tomokazu Sasaki,[1] Yasukazu Saito,[1]
Hiroaki Hatori, and Tadayoshi Tanaka[2]

National Institute of Advanced Industrial Science and Technology (AIST), 16-1, Onogawa, Tsukuba, Ibaraki 305-8569

[1]Faculty of Engineering, Tokyo University of Science, 1-3, Kagurazaka, Shinjuku-ku, Tokyo 162-8601

[2]Ibaraki Industrial Technology Institute, 3781-1, Nagaoka, Ibaraki-cho, Higashi-Ibaraki-Gun, Ibaraki 311-3195

Received March 5, 2004; E-mail: ando-yuji@aist.go.jp

A thermally regenerative fuel cell, converting low-quality heat at around 100 °C directly into electric power, is composed of a redox reaction pair of acetone hydrogenation and 2-propanol dehydrogenation. The magnitude of its open-circuit voltage (V_{OC}) was determined by the Gibbs energy change of acetone hydrogenation, without exhibiting activation polarization. Its short-circuit current (I_{SC}) was insensitive to the extents of catalyst loading at the anode, in contrast to the cathode, because acetone hydrogenation proceeded more slowly than hydrogen dissociation. The I_{SC} characteristics were improved with increasing sulfuric acid concentrations at the cathode, which would have resulted from the rate enhancement of acetone reduction due to more abundant protons usable at the catalyst sites. Both V_{OC} and I_{SC} of the fuel cell were increased along with increasing the acetone/2-propanol ratio in the catholyte, suggesting favorable effects of the thermodynamical acetone activity and the coverage increment of acetone at the same cathode catalyst sites.

A 2-propanol/acetone/hydrogen chemical heat pump system for upgrading low-quality heat from 80 °C to useful heat at 200 °C had previously been proposed (Eqs. 1 and 2).[1] Catalytic 2-propanol dehydrogenation (Eq. 1) was studied under boiling and refluxing conditions with suspended copper chromite,[2] Raney nickel,[3] nickel boride,[4] nickel fine particles prepared with a gas-evaporation technique,[5] carbon-supported ruthenium,[6] and ruthenium–platinum composite metal (Ru–Pt/carbon).[7,8]

$$(\mathrm{CH_3})_2\mathrm{CHOH(l)} \longrightarrow (\mathrm{CH_3})_2\mathrm{CO(g)} + \mathrm{H_2(g)}, \qquad (1)$$

$$(\text{endotherm: } \Delta H^\circ = 100.4\ \text{kJ/mol})$$

$$(\mathrm{CH_3})_2\mathrm{CO(g)} + \mathrm{H_2(g)} \longrightarrow (\mathrm{CH_3})_2\mathrm{CHOH(g)}. \qquad (2)$$

$$(\text{exotherm: } \Delta H^\circ = -55.0\ \text{kJ/mol})$$

Provided that the redox reaction of acetone hydrogenation proceeded electrocatalytically (Eqs. 3 and 4), a new thermally regenerative fuel cell, converting low-quality heat into electric energy directly, could be constructed by coupling it to the well-established thermo-reaction of catalytic 2-propanol dehydrogenation (Eq. 1).[9,10]

At the anode, hydrogen dissociates into protons and electrons,

$$\mathrm{H_2(g)} \longrightarrow 2\mathrm{H^+} + 2\mathrm{e^-}, \qquad (3)$$

whereas acetone, protons and electrons react electrochemically at the cathode,

$$(\mathrm{CH_3})_2\mathrm{CO(l)} + 2\mathrm{H^+} + 2\mathrm{e^-} \longrightarrow (\mathrm{CH_3})_2\mathrm{CHOH(l)}. \qquad (4)$$

The outlet solution from the cathode is supplied to a regenerator, in which acetone and hydrogen gas are reproducible thermo-catalytically. A schematic diagram of an acetone/hydrogen-based thermally regenerative fuel cell is shown in Fig. 1.

In order to examine and enhance the I–V characteristics of the acetone/hydrogen-based thermally regenerative fuel cell, detailed studies on electrocatalytic processes of acetone hydrogenation at the cathode were attempted in the present study.

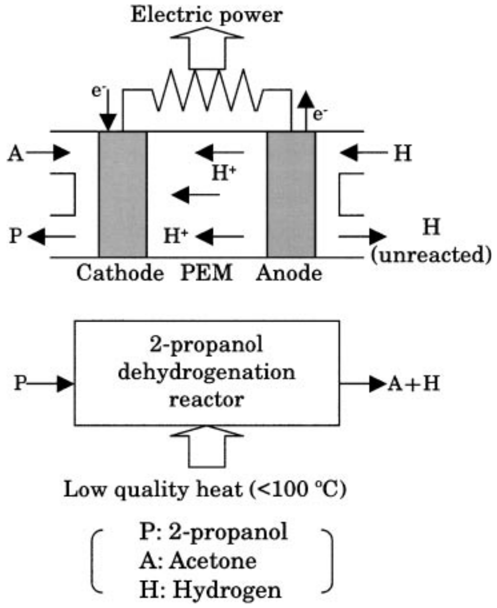

Fig. 1. A schematic diagram of acetone/hydrogen-based thermally regenerative fuel cell.

Published on the web October 9, 2004; DOI 10.1246/bcsj.77.1855

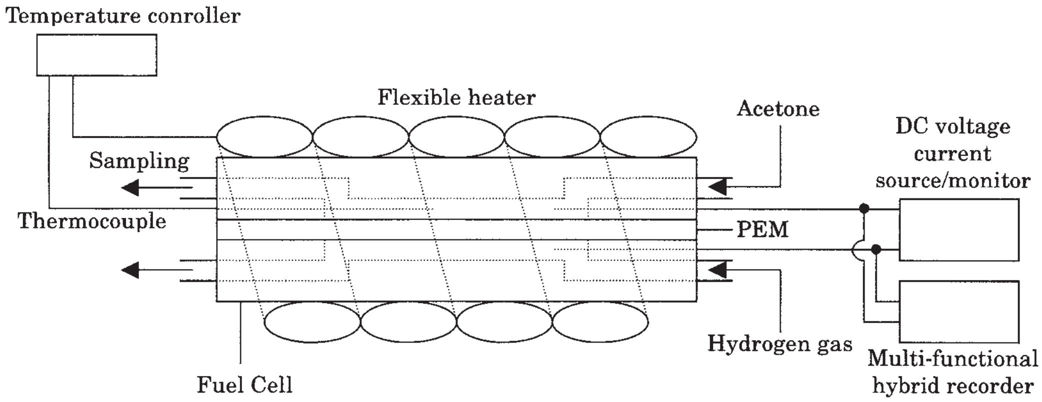

Fig. 2. A schematic diagram of the experimental setup.

Experimental

Preparation of a Carbon-Supported Electrode Catalyst. We prepared carbon-supported Ru–Pt composite catalysts in the following manner. In the first place, carbon-cloth (Kuraray Co., CH720-25 and CH900-25) was impregnated at room temperature with aqueous solutions of $RuCl_3 \cdot 3H_2O$ and K_2PtCl_4 mixed at a weight ratio of Ru/Pt = 1/1, and then evacuated at 343 K for 10 h. The impregnated carbon-cloth was reduced by gaseous hydrogen at 573 K for 12 h, followed by filtration, washing with a large amount of water and evacuating at 343 K for 10 h. CH720-25 and CH900-25 are made of the same carbon material, but CH720-25 has almost twice the thickness of CH900-25, or weight per unit area.

Electrochemical Measurements of the I–V Characteristics on an Acetone-Hydrogen-Based Fuel Cell. A schematic diagram of the experimental setup is shown in Fig. 2. A commercially available DC voltage current source/monitor (Advantest Co., R6243) was used to monitor the electric output of the experimental fuel cell. The electromotive forces as well as temperatures inside the fuel cell were measured continuously with a multi-functional hybrid recorder (Chino Co., Al 3000). A cell with a 2 × 2 cm^2 area was heated at 333 K, or other prescribed temperatures, by a flexible heater as a whole, being set with a temperature controller (Iuchi Co., TX-300). The electrode pair was separated with a polymer electrolyte membrane (Du Pont Co., Nafion® 117). Hydrogen gas was supplied at 0.1 MPa to the anode at a rate of 50 mL/min, whereas a mixture of acetone, 2-propnaol, and water was supplied at a rate of 1 mL/min to the cathode in order to avoid any change in the acetone/2-propanol ratio in the catholyte during the reaction, and for affording enough protons to the polymer electrolyte membrane. In order to vary the concentrations of protons, sulfuric acid aqueous solutions were fed to the cathode in some experiments.

Results and Discussion

Effect of the Reaction Temperature on the I–V Characteristics. The I–V characteristics of the fuel cell were obtained by the electrode catalysts of Ru–Pt/carbon-cloth (CH900-25), consisting of the cathode (26 wt % loading) fed with a mixture solution (acetone:2-propanol:pure water = 10:10:80) and the anode (10 wt %) with hydrogen.

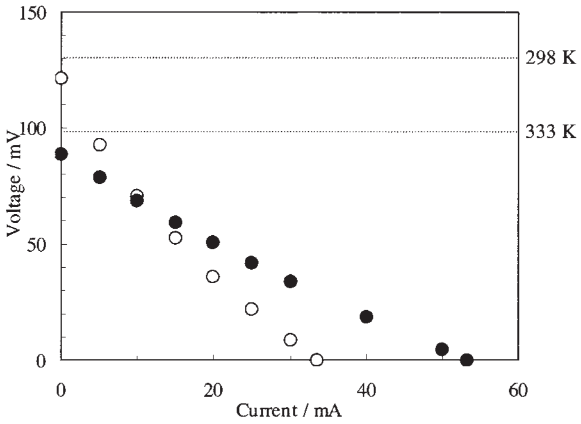

Fig. 3. Effect of reaction temperature on I–V characteristics of the fuel cell. The mixture solution (acetone:2-propanol:pure water = 10:10:80) was fed to the cathode. Reaction temperature of 298 K (○) and 333 K (●).

As shown in Fig. 3, a linear relationship in I–V characteristics is evident, whereas the temperature dependences are opposite between the open-circuit voltage (V_{OC}) and the short-circuit current (I_{SC}). The tendency of a larger magnitude of V_{OC} at a lower reaction temperature should be regulated by the standard Gibbs energy change (ΔG°) of acetone hydrogenation, reflecting the equilibrium of hydrogenation favored at low temperatures (Fig. 4). The magnitudes of V_{OC} were slightly smaller than those calculated from ΔG° of acetone hydrogenation, probably because the thermodynamic activity of acetone in the feed solution was inferior to neat, and a certain extent of acetone crossover to the anode was inevitable.

With regard to the magnitudes of I_{SC}, its kinetical nature would be affected by the reaction temperature, since the rates of acetone reduction at the cathode and of proton transfer through the polymer electrode membrane are decisive to them in this fuel cell.

Effect of Catalyst Loading on the I–V Characteristics. In order to correlate the magnitudes of I_{SC} with the rates of the hydrogenation reaction and mass transfer, the catalyst amounts of Ru–Pt for the anode and the cathode were varied independently, as shown in Fig. 5. The I–V characteristics of the fuel cell were obtained with the electrode catalysts of Ru–Pt/carbon-cloth (CH720-25) by varying the amounts of catalyst loading, where the mixture solution (acetone:2-propanol:pure water = 5:5:90) was fed to the cathode and hydrogen to the anode. A set of 2 wt % at the anode and 10 wt % at the

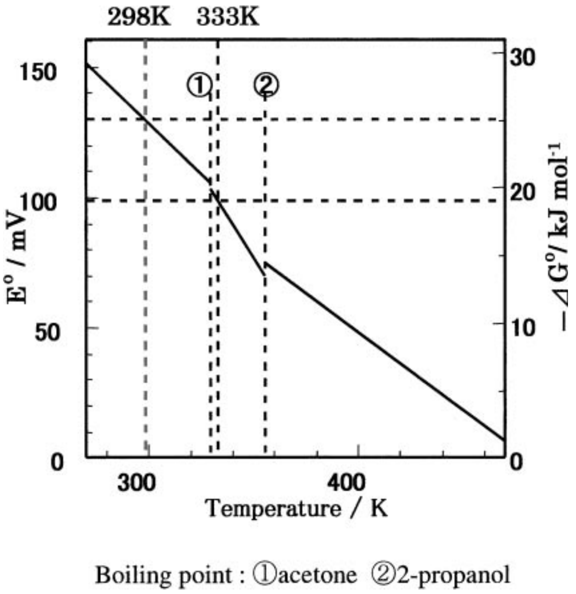

Fig. 4. Relationship between reaction temperature and the standard Gibbs energy of acetone hydrogenation.

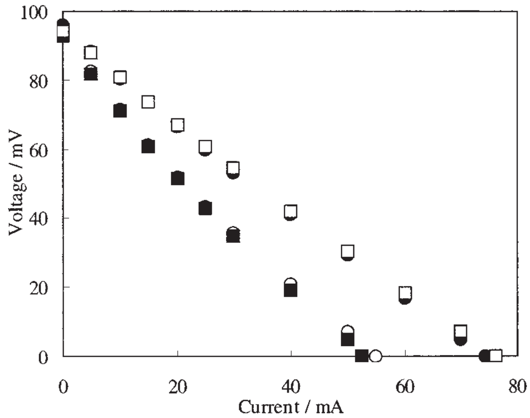

Fig. 5. Effect of catalyst loading on I–V characteristics of the fuel cell. The mixture solution (acetone:2-propanol: pure water = 5:5:90) was fed to the cathode. The set of 2 wt % at the anode and 10 wt % at the cathode (●), 10–10 (□), 10–2 (○), and 2–2 (■).

cathode (referred as 2–10 hereafter) was evidently superior to the sets of 2–2 and 10–2. Moreover, the set of 10–10 performed similarly to the 2–10 set. Provided that the reaction yielding protons and electrons at the anode proceeded far more rapidly than the reaction of acetone reduction at the cathode, the extent of catalyst loadings at the anode would be indifferent to the magnitude of I_{SC}, in contrast to the case of the cathode. A hypothetical assumption of slow acetone hydrogenation at the cathode should allow for the extent of catalyst loadings to be sensitive to the I_{SC} magnitudes. Improvements of electrode catalysts are certainly required at the cathode side.

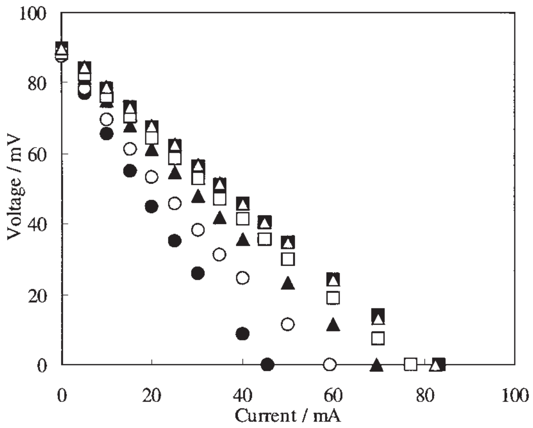

Fig. 6. Effect of sulfuric acid concentration at the cathode on I–V characteristics of the fuel cell. The mixture solution (acetone:2-propanol:sulfuric acid aqueous solution = 10:10:80) was fed to the cathode. Sulfuric acid concentration of 50.0 mmol/L (△), 25.0 (■), 12.5 (□), 5.0 (▲), 0.625 (○), and 0.0 (●).

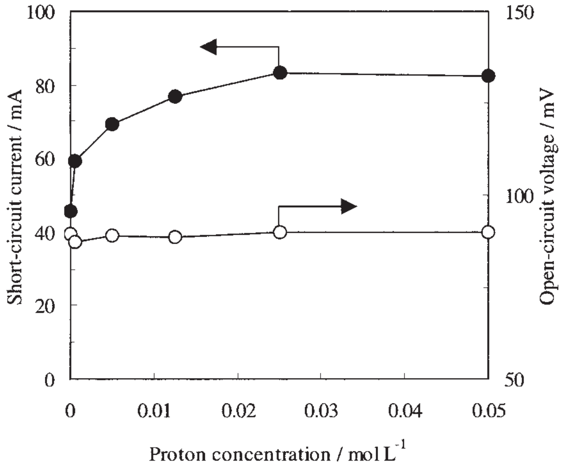

Fig. 7. Effect of sulfuric acid concentration at the cathode on short-circuit current and open-circuit voltage of the fuel cell.

Effect of the Proton Concentration on the I–V Characteristics at the Cathode. The proton concentrations at the cathode are controllable in the present fuel cell by adding acid to the aqueous acetone solution. The I–V characteristics with using 10 wt % Ru–Pt/carbon-cloth (CH900-25) at both electrodes of various proton concentrations at the cathode are shown in Fig. 6 by feeding prescribed amounts of the mixture solution (acetone:2-propanol:sulfuric acid aqueous solution = 10:10:80) to the cathode side. In Fig. 7, I_{SC} and V_{OC} are plotted as a function of the sulfuric acid concentration at the cathode. Apparently, the fuel cell performance was improved along with the sulfuric acid concentration. The magnitudes of I_{SC} converged at a sulfuric acid concentration of 25.0 mmol/L to its highest value of 83 mA, whereas V_{OC} was constant irrespective of the sulfuric acid concentrations. No byproducts were detected from the solution, which was examined at the cathode outlet.

The increment of I_{SC} would result from an enhanced reduction rate of acetone, since the electrochemical process was a relatively slow step at the cathode. Any protonation process on the catalyst surface at the cathode would improve the I–V characteristics of the cell. The limiting sulfuric acid concentration of 25.0 mmol/L may correspond to the saturated amount

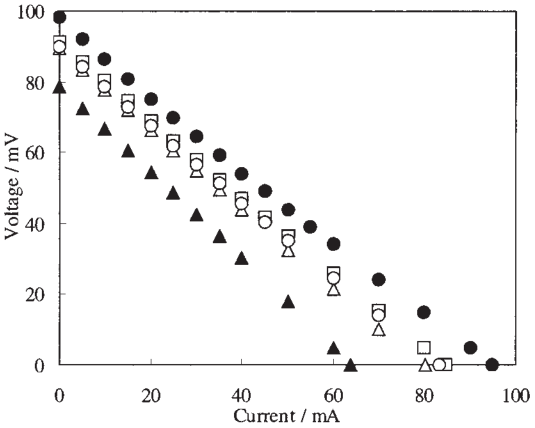

Fig. 8. Effect of composition of catholyte on I–V characteristics of the fuel cell. Composition shown in Table 1 of I (○), II (▲), III (●), IV (□), and V (△).

Table 1. Composition of Catholyte

Components	Composition/vol %				
	I	II	III	IV	V
Acetone	10	5	15	5	20
2-Propanol	10	15	5	5	20
0.1 mol/L H_2SO_{4aq}	20	20	20	20	20
H_2O	60	60	60	70	40

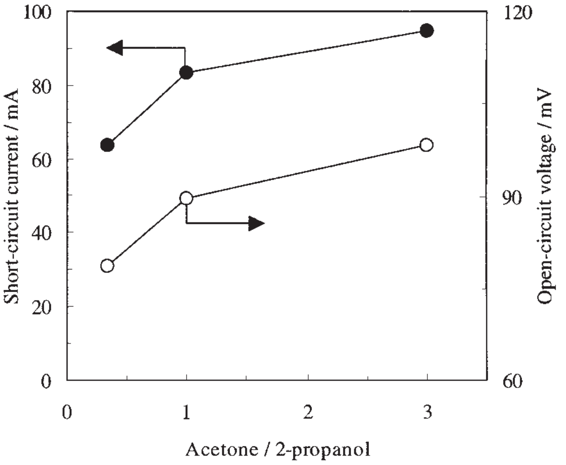

Fig. 9. Effect of acetone/2-propnaol ratio in catholyte on short-circuit current and open-circuit voltage of the fuel cell.

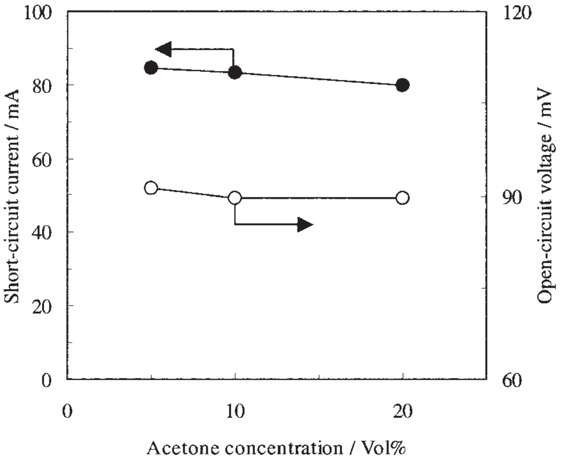

Fig. 10. Effect of acetone concentration in catholyte on short-circuit current and open-circuit voltage of the fuel cell.

of protons for adsorbed acetone at the cathode. It is to be noted that both the acetone coverage over the catalyst and, consequently, the electrochemical potential at the cathode are unaffected by sulfuric acid, which would be the reason why the sulfuric acid concentrations in the catholyte were indifferent to the magnitude of V_{OC}.

The converged high I_{SC} value of 83 mA was equivalent to the value reported in previous work with the use of 30 wt % Ru–Pt/carbon-cloth at both electrodes.[10] It is noteworthy that the highest I_{SC} was achieved in the present work using a far smaller amount of catalyst metal than in the previous work.

Effect of the Composition of Catholyte on the I–V Characteristics. The concentration ratio of acetone to 2-propanol in catholyte is another controllable factor for this fuel cell. As shown in Fig. 8, the I–V characteristics were changed with the catholyte compositions, where 10 wt % Ru–Pt/carbon-cloth (CH900-25) at both electrodes, hydrogen feed to the anode and the fraction of sulfuric acid in the catholyte were kept constant. The catholyte compositions are summarized in Table 1. I_{SC} and V_{OC} were depicted as a function either of the acetone/2-propanol molar ratios at a constant fraction of water (Fig. 9) or of the acetone concentrations, which keeping the acetone/2-propanol ratio to be unity (Fig. 10) in the catholyte. It is evident that the magnitudes of I_{SC} and V_{OC} increased along with the acetone/2-propanol ratio, whereas the acetone concentration, itself, is unimportant in the catholyte, as long as the equimolar mixture of acetone and 2-propanol is adopted. Provided that acetone and 2-propanol are adsorbed onto the cathode catalyst competitively, the acetone coverage, and consequently the magnitudes of V_{OC}, would be sensitively affected by the acetone/2-propanol ratio in the catholyte. These tendencies observed on V_{OC} were similar to the cases of I_{SC}, since the rate processes in this fuel cell were determined with the common factor of the acetone coverage on the cathode catalyst at a constant proton concentration.

Reaction Mechanism of Electrochemical Acetone Hydrogenation on the Cathode. In the conventional oxygen/hydrogen fuel cell, a large voltage drop is inevitable due to activation polarization during the four-electron reduction of molecular oxygen at the cathode. On the contrary, no clear voltage drop was detected in the present fuel cell, even at the low current range, as is apparent in Figs. 5, 6, and 8. No difficulty seems to arise in the electrochemical acetone reduction on the cathode. The voltage drop in the present cell, throughout the current range, would be due to resistance polarization, since I_{SC} of this fuel cell is much smaller than that of the conventional oxygen/hydrogen fuel cell, and mass transfer must not be the rate-determining step within the current value in the experiments.

Tohrizawa et al. suggested a mechanism of acetone hydrogenation at the cathode catalyst of an acetone/hydrogen fuel cell, where difficult C–H bond formation at the 2-propanol methine group was assumed among facile sequences from a catalytic viewpoint.[11] Since the important roles of protons and the adsorbed acetone have been elucidated in the present study, a detailed reaction mechanism may be proposed based on an improved I_{SC} with increasing sulfuric acid concentration and acetone coverage on the surface, where protonation of the carbanion to form the methine C–H bond is designated as the most important step throughout the reaction.

Conclusion

In this study, we have examined several factors that promote electrocatalytic acetone hydrogenation at the cathode in order to enhance the I–V characteristics of an acetone/hydrogen-based thermally regenerative fuel cell. The following results were obtained from the experiments:

(1) As indicated from the standard Gibbs energy change of acetone hydrogenation, larger magnitudes of open-circuit voltage were observed at lower reaction temperatures.

(2) Based on the catalyst-loading dependence on the I–V characteristics, the dominated kinetic process in this cell was found to be the step of acetone hydrogenation at the cathode.

(3) High proton concentrations introduced from sulfuric acid to the catholyte could enhance the rate of electrocatalytic acetone reduction at the cathode.

(4) Enlarged acetone/2-propanol ratios in the catholyte resulted in increments of both I_{SC} and V_{OC}, which would be ascribed to a larger acetone coverage on the cathode catalyst of the fuel cell.

(5) No voltage drop, except for resistance polarization, was observed all through the current range in the present cell, indicating rapid protonation and facile two-electron transfer toward acetone.

(6) A reaction mechanism was proposed, where the most important step throughout the reaction was protonation of the carbanion for yielding the methine C–H bond.

References

1 Y. Saito, H. Kameyama, and K. Yoshida, *Int. J. Energy Res.*, **11**, 549 (1987).

2 F. Clase and J. C. Junger, *Bull. Soc. Chim. Fr., Ser. 5*, **25**, 1167 (1958).

3 F. Velasco, *Chim. Ind. (Milan)*, **81**, 521 (1959).

4 D. E. Mears and M. Boudart, *AIChE J.*, **12**, 313 (1966).

5 M. Noda, S. Shinoda, and Y. Saito, *J. Chem. Soc. Jpn.*, **1984**, 1017; M. Noda, S. Shinoda, and Y. Saito, *Bull. Chem. Soc. Jpn.*, **61**, 961, 3421 (1988).

6 M. Yamashita, T. Kawamura, M. Suzuki, and Y. Saito, *Bull. Chem. Soc. Jpn.*, **64**, 272 (1991).

7 E. Ito, M. Yamashita, S. Hagiwara, and Y. Saito, *Chem. Lett.*, **1991**, 351.

8 Y. Ando, M. Yamashita, and Y. Saito, *Bull. Chem. Soc. Jpn.*, **76**, 2045 (2003).

9 Y. Ando, T. Tanaka, T. Doi, and T. Takashima, *Energy Convers. Manage.*, **42**, 1807 (2001).

10 Y. Ando, T. Tanaka, and M. Amano, *Energy Convers. Manage.*, **44**, 2811 (2003).

11 R. Tohrizawa, Y. Kimura, Y. Saito, Y. Ando, and T. Tanaka, *J. Hydrogen Energy Syst. Soc. Jpn.*, **24**, 31 (1999).